Low-temperature (<200 $^{\circ}$C) solid-phase crystallization of high substitutional Sn concentration (~10%) GeSn on insulator enhanced by weak laser irradiation

Kenta Moto, Takayuki Sugino, Ryo Matsumura, Hiroshi Ikenoue, Masanobu Miyao, and Taizoh Sadoh

Citation: AIP Advances **7**, 075204 (2017); doi: 10.1063/1.4993220
View online: http://dx.doi.org/10.1063/1.4993220
View Table of Contents: http://aip.scitation.org/toc/adv/7/7
Published by the American Institute of Physics

HAVE YOU HEARD?
Employers hiring scientists and engineers trust
PHYSICS TODAY | JOBS
www.physicstoday.org/jobs

AIP ADVANCES 7, 075204 (2017)

Low-temperature (<200 °C) solid-phase crystallization of high substitutional Sn concentration (~10%) GeSn on insulator enhanced by weak laser irradiation

Kenta Moto,[1] Takayuki Sugino,[1] Ryo Matsumura,[1,2] Hiroshi Ikenoue,[3] Masanobu Miyao,[1] and Taizoh Sadoh[1,a]
[1]*Department of Electronics, Kyushu University, 744 Motooka, Fukuoka 819-0395, Japan*
[2]*JSPS, 5-3-1 Kojimachi, Chiyoda-ku, Tokyo 102-0083, Japan*
[3]*Department of Gigaphoton Next GLP, Kyushu University, 744 Motooka, Fukuoka 819-0395, Japan*

(Received 21 March 2017; accepted 30 June 2017; published online 12 July 2017)

Low temperature (<200 °C) crystallization of GeSn (substitutional Sn concentration: >8%) on insulating substrates is essential to realize next generation flexible electronics. To achieve this, a growth method of high quality GeSn films on insulating substrates by combination of laser irradiation and subsequent thermal annealing is developed. Here, the laser fluence is chosen as weak, which is below the critical fluence for crystallization of GeSn. It is clarified that for samples irradiated with weak laser fluence, complete crystallization of GeSn films is achieved by subsequent thermal annealing at ~170 °C without incubation time. In addition, the quality of GeSn films obtained by this method is higher compared with conventional growth techniques such as melting growth by pulsed laser annealing or solid-phase crystallization (SPC) without pre-laser irradiation. Substitutional Sn concentrations in the grown layers estimated by Raman spectroscopy measurements are 8-10%, which far exceed thermal equilibrium solid-solubility of Sn in Ge (~2%). These phenomena are explained by generation of a limited number of nuclei by weak laser irradiation and lateral SPC by subsequent thermal annealing. This method will facilitate realization of next-generation high performance devices on flexible insulating substrates. © *2017 Author(s). All article content, except where otherwise noted, is licensed under a Creative Commons Attribution (CC BY) license (http://creativecommons.org/licenses/by/4.0/).* [http://dx.doi.org/10.1063/1.4993220]

GeSn crystals (substitutional Sn concentration: >8%) on insulator structures are strongly desired to realize high-speed thin film transistors (TFTs) and high-efficiency optical devices for next generation electronics. This is because GeSn crystals have higher carrier mobility than Si and Ge due to the direct-transition energy band structure with smaller effective mass of carriers for high substitutional Sn concentrations (>8%).[1,2] For the device application on low cost plastic substrates such as polyethylene terephthalate (softening temperature: ~200 °C), development of a low temperature (<200 °C) growth method of GeSn crystals (substitutional Sn concentration: >8%) on insulating substrates is essential.

To date, various growth methods of GeSn have been investigated. However, most of the researches are related to epitaxial growth of GeSn on crystalline substrates (c-Si and c-Ge) using molecular beam epitaxy[3–5] and chemical vapor deposition.[4,6–8] On the other hand, reports of GeSn growth on insulating substrates are limited.[9–14] Here, to obtain GeSn crystals on insulating substrates, solid phase crystallization (SPC)[9–12] and melting growth by pulsed laser annealing (PLA),[13,14] have been investigated. We reported SPC of amorphous GeSn (a-GeSn) films with initial Sn concentration of 20% at a low temperature (<200 °C).[15] This enabled formation of GeSn films having high substitutional Sn

[a]Electronic mail: sadoh@ed.kyushu-u.ac.jp

 © Author(s) 2017

concentration (~10%). This value exceeded thermal equilibrium solid-solubility of Sn in Ge (~2%).[16] However, long time annealing was necessary, e.g., ~100 h at 180 °C,[15] to obtain sufficiently large growth length (~100 μm) for device application. This indicates that reduction of SPC processing time is necessary for practical application.

On the other hand, PLA is expected to induce non-thermal equilibrium growth by rapid cooling, where crystallization proceeds in a very short time. Recently, we reported PLA of a-GeSn films on insulator.[14] This enabled crystallization of GeSn having high substitutional Sn concentration (~12%). However, surface roughness induced by melting in PLA was a big problem for device application.

Under such background, we focus on PLA with low fluence to prevent from melting. By combining the weak PLA and SPC, formation of GeSn crystals with high substitutional Sn concentration and flat surface is expected. In the present study, we investigate growth characteristics of GeSn films on insulator by laser irradiation with a wide range of laser fluence and subsequent thermal annealing at low temperatures. It is revealed that weak laser irradiation (10-100 mJ/cm^2) to a-GeSn films significantly reduces the processing time for complete crystallization by subsequent low-temperature annealing (≤200°C). The grown GeSn films have higher quality compared with PLA by melting (fluence: 110-170 mJ/cm^2) or conventional SPC. The growth mechanism of the high-quality GeSn films is discussed on the basis of a limited number of nuclei induced by weak laser irradiation.

The experimental procedure is schematically shown in Fig. 1. Amorphous-$Ge_{0.8}Sn_{0.2}$ films (thickness: 100 nm) were deposited on quartz substrates at room temperature by a molecular-beam deposition system with a base pressure of ~5×10^{-10} Torr. These samples were irradiated with a KrF excimer laser (wavelength: 248 nm, pulse duration: 80 ns, repetition rate: 100 Hz, irradiation number of pulses: 100 shots, beam size: 360 μm × 500 μm) with a wide range of fluence per pulse (10–170 mJ/cm^2) in air. Subsequently, the samples were annealed (150–200 °C, 5 min–25 h) in dry nitrogen ambient. Crystalline qualities of the GeSn layers irradiated with various fluence and annealed at various temperatures were analyzed by using micro-probe Raman scattering spectroscopy (excitation laser wavelength: 532 nm, laser beam spot diameter: ~1 μm).

Raman scattering measurements are performed for samples before and after laser irradiation (pulse number: 100 shots). Typical Raman spectra are shown in Fig. 2(a), where laser fluence per pulse was chosen as 10 and 110 mJ/cm^2, respectively, where the Raman measurements were performed from the top side of the samples. Here, the spectral intensity is normalized by the Raman peak intensity of a crystalline Ge substrate. After irradiation with fluence of 10 mJ/cm^2, a weak and broad peak has emerged at 283.0 cm^{-1}, where the full width at half maximum (FWHM) is 17.7 cm^{-1}. Such weak and broad features suggest that this peak is originated from Ge-Ge bonding in not crystalline GeSn but amorphous GeSn, where the amorphicity is modulated by laser irradiation. On the other hand, for the sample irradiated with 110 mJ/cm^2, a sharp peak (FWHM: 6.6 cm^{-1}) due to Ge-Ge bonding in crystalline GeSn has appeared at 294.0 cm^{-1}, suggesting crystallization by laser irradiation. The values of the intensity of the Raman peaks due to Ge-Ge bonding are summarized in Fig. 2(b) as a function of the laser fluence. In the low fluence region (10-100 mJ/cm^2), they increase with increasing laser fluence. Coincidently, the values of FWHM decreased from 17.7 cm^{-1} (10 mJ/cm^2) to 8.8 cm^{-1} (60 mJ/cm^2) and 7.2 cm^{-1} (100 mJ/cm^2) (not shown). In addition, Raman peak positions of Ge-Ge peaks were 283.0 cm^{-1} (10 mJ/cm^2), 289.0 cm^{-1} (60 mJ/cm^2) and 292.5 cm^{-1} (100 mJ/cm^2) (not shown). Here, in-situ reflectance measurements revealed that the samples surfaces were not melted during laser irradiation (not shown). The changes in the intensities, FWHM, and positions of the

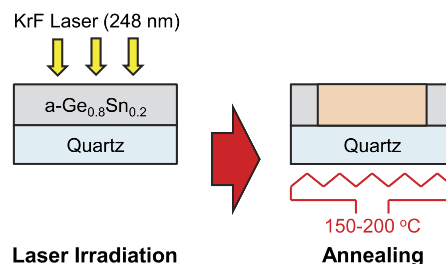

FIG. 1. Schematic experimental procedure.

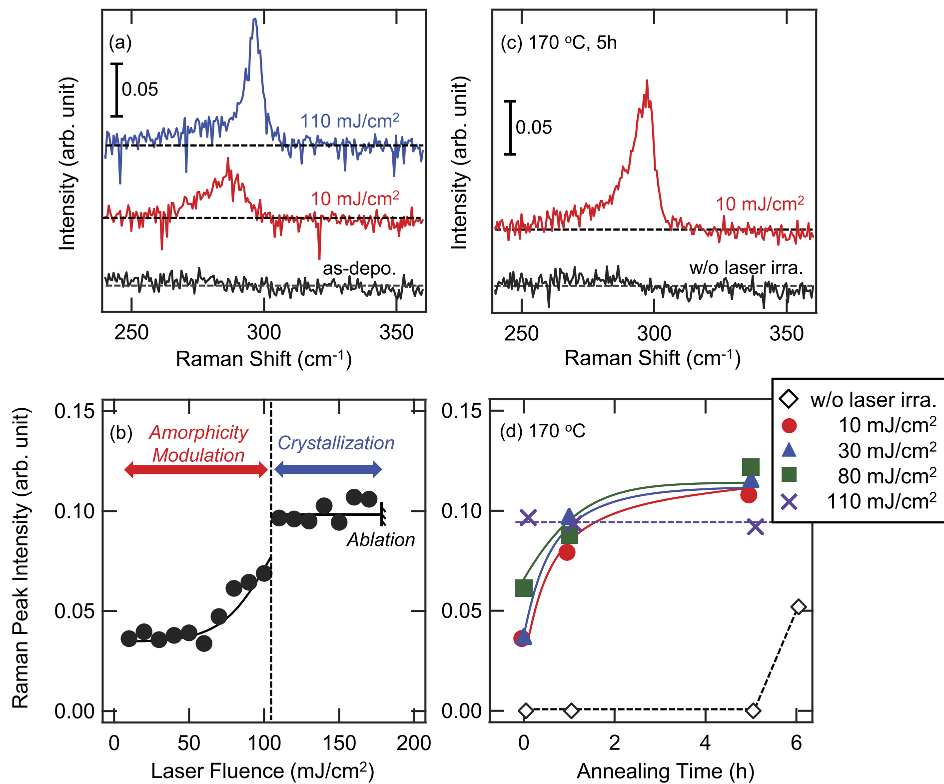

FIG. 2. (a) Raman spectra of $Ge_{0.8}Sn_{0.2}$ samples (thickness: 100 nm) before and after laser irradiation with fluence of 10 and 110 mJ/cm^2. (b) Laser fluence dependence of the intensity of Raman peak due to Ge-Ge bonding. (c) Raman spectra after annealing (170 °C, 5h) with and without pre-laser irradiation (10 mJ/cm^2). (d) Annealing time dependence of the Raman peak intensity for samples with and without laser irradiation at different fluence (10, 30, 80, 110 mJ/cm^2). The Raman spectral intensity is normalized by the Raman peak intensity of a crystalline Ge substrate. Base lines of Raman spectra are shown as broken lines in (a) and (c).

Raman peaks in this fluence region are speculated to be caused by densification of a-GeSn films through amorphicity modulation by weak laser irradiation (fluence: 10-100 mJ/cm^2). In the medium fluence (110-170 mJ/cm^2), the values of intensity saturate as shown in Fig. 2(b), where the values of FWHM decreased to 5.5 cm^{-1} (170 mJ/cm^2) (not shown). This indicates crystallization occurs in this medium fluence region. Finally, in the high fluence region (>170 mJ/cm^2), ablation of the GeSn films occurred. In-situ reflectance measurements revealed melting of the surface regions of the samples for fluence above 100 mJ/cm^2 (not shown).

We investigate effects of thermal annealing for samples after laser irradiation. Raman spectra obtained after the laser irradiation (10 mJ/cm^2) and subsequent annealing (170 °C, 5 h) are shown in Fig. 2(c). In this figure, Raman spectra for the sample after annealing (170 °C, 5 h) without laser irradiation are also shown. Interestingly, the intensity of the Raman peak for the sample irradiated with low fluence (10 mJ/cm^2) is significantly increased by annealing. On the other hand, no Raman peak is observed for the sample without laser irradiation even after annealing. To investigate laser fluence dependence of these phenomena, the intensity of the Raman peaks due to Ge-Ge bonding for samples with and without laser irradiation under different fluence (10, 30, 80, 110 mJ/cm^2) are summarized in Fig. 2(d) as a function of the annealing time (170 °C). In low fluence region (10, 30, 80 mJ/cm^2), the intensity of the Raman peaks sharply increase in a short annealing time (~1 h) without incubation time and reach saturation at ~5 h, indicating completion of SPC of GeSn films by annealing (~5 h). In the medium fluence region (110 mJ/cm^2), the intensity of Raman peaks is hardly changed by annealing. The saturated values of the Raman peak intensity of samples irradiated with low fluence (10, 30, 80 mJ/cm^2) exceeded those of samples irradiated with medium fluence (110 mJ/cm^2), i.e., the conventional PLA with melting. This indicates that the grown layer obtained by weak laser irradiation

and subsequent annealing have higher quality than those obtained by conventional PLA. As a result, weak laser irradiation (fluence: 10-100 mJ/cm^2) enables formation of high quality GeSn films in a short annealing time at a low temperature (170 ^{o}C).

We also performed Raman measurements from the back side of the samples through transparent substrates, as well as the top side of the samples. The results of the Raman measurements from the back side indicated that the minimum laser fluence to observe a weak and broad Raman peak suggesting amorphicity modulation was about 40 mJ/cm^2, which was larger by about 30 mJ/cm^2 than that for the top side observation (10 mJ/cm^2), as shown in Fig. 2(a). Here, the detection depth of the Raman measurements is about 20 nm in the present study (excitation laser wavelength: 532 nm).[17] This difference is attributed to the shallow penetration depth (5-10 nm) of KrF excimer laser irradiation (wavelength: 248 nm).[17] On the other hand, after subsequent annealing for 5 h (170 ^{o}C), the positions and FWHM of the Raman peaks observed from the back side became almost the same as those from the top side. This suggests almost uniform crystal structures in the depth direction for GeSn films grown by weak laser irradiation and subsequent low temperature annealing. Further investigation is needed to clarify the detail.

Annealing characteristics of the Raman peak intensity are investigated at different annealing temperatures (150-200 ^{o}C). The results of samples with and without laser irradiation are shown in Figs. 3(a) and 3(b), respectively, where the Raman measurements were performed from the top side of the samples. Here, the laser fluence was chosen to obtain almost identical Raman peak intensity (~0.05) after irradiation. For the samples subjected to laser irradiation, the characteristics are divided into two groups depending on the annealing temperature, i.e., 150 ^{o}C and 170-200 ^{o}C. At the former annealing temperature (150 ^{o}C), the intensity slowly increases with increasing annealing time without incubation time, and reaches saturation at ~15 h. On the other hand, at the latter annealing temperature (170-200 ^{o}C), the intensities rapidly increase with increasing annealing time without incubation time and saturate in short annealing times (1-5 h). It is noted that the saturated values of the Raman peak intensity for samples annealed at 170-200 ^{o}C are approximately twice of that at 150 ^{o}C. This phenomenon is speculated to be originated from large crystal grains in samples annealed at 170-200 ^{o}C, which is attributed to lateral SPC from a small number of nuclei generated by amorphicity modulation. These annealing temperature dependent growth mechanisms will be discussed later (see Fig. 4). On the other hand, in the samples without laser irradiation [Fig. 3(b)], i.e., conventional SPC, growth is initiated after incubation times for nucleation. After the incubation times, the Raman

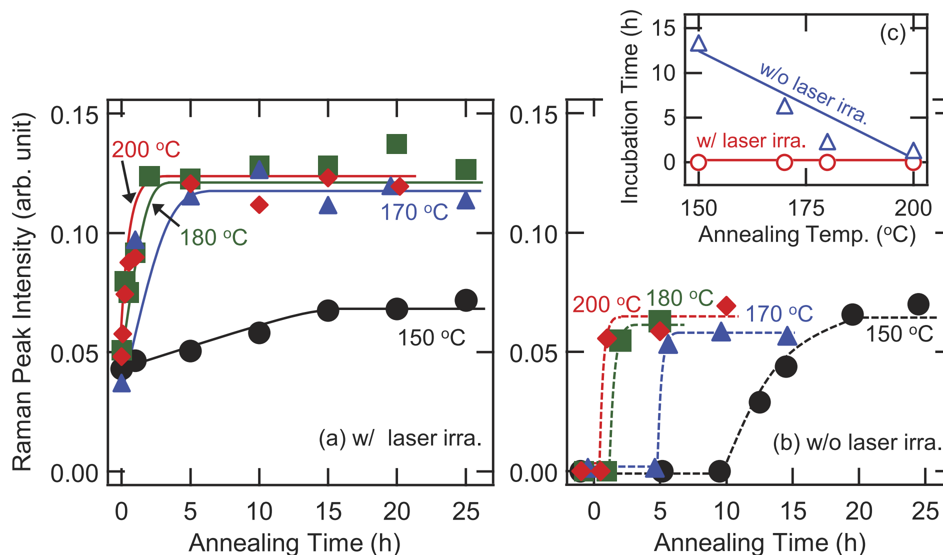

FIG. 3. Annealing characteristics of the Raman peak intensity for $Ge_{0.8}Sn_{0.2}$ samples (thickness: 100 nm) at different temperatures (150, 170, 180, 200 ^{o}C) with (a) and without pre-laser irradiation (b). (c) Incubation time for nucleation in samples with and without laser irradiation as a function of annealing temperature. Raman spectral intensity is normalized by the Raman peak intensity of a crystalline Ge substrate.

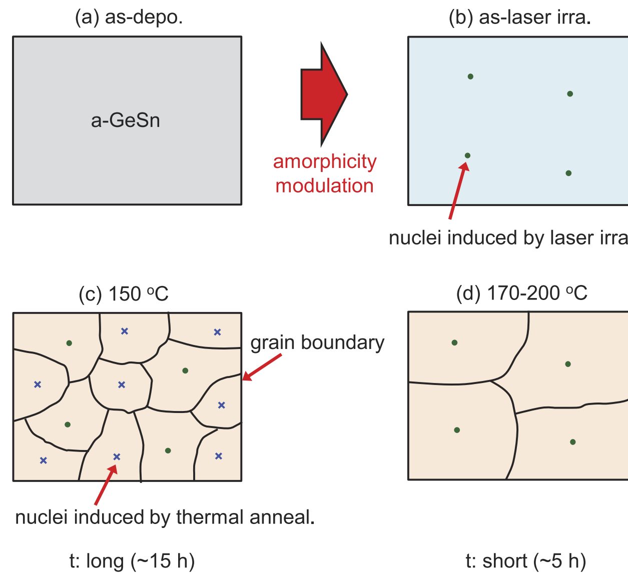

FIG. 4. Schematics of crystal structures in $Ge_{0.8}Sn_{0.2}$ samples before (a) and after weak laser irradiation (fluence: 10-100 mJ/cm^2) (b), and after subsequent annealing at 150 °C (~15 h) (c) and 170-200 °C (~5 h) (d).

peak intensity increases with increasing annealing time and reaches saturation with almost identical values for all annealing temperatures (150-200 °C). The incubation times for samples with and without laser irradiation are summarized in Fig. 3(c) as a function of the annealing temperature. The incubation times for samples without laser irradiation become long with decreasing annealing temperature, which shows a good agreement with the previous reports of conventional SPC of $Si_{1-x}Ge_x$($0<x<1$).[18–20] In other words, laser irradiation with low fluence is very effective to enhance SPC by subsequent thermal annealing at low temperatures (150-200 °C).

The substitutional Sn concentrations in grown layers for samples after weak laser irradiation (10-100 mJ/cm^2) and subsequent annealing (170-200 °C) were evaluated from the Raman peak positions.[21,22] The substitutional Sn concentrations were 8-10% just after completion of crystallization (~5 h), and these values were hardly changed after additional long time annealing (~20 h). These results indicate that grown GeSn has high substitutional Sn concentrations with high thermal stability. This method of weak laser irradiation and subsequent thermal annealing is useful to realize high speed TFTs and high efficiency optical devices.

To analyze detailed quality of GeSn crystals, FWHM of Raman peaks was evaluated. The values of FWHM for grown samples (annealing temperature: 170-200 °C) with and without laser irradiation were 7.5-8.5 cm^{-1} and 9.2-9.6 cm^{-1}, respectively. Here, the substitutional Sn concentrations were almost the same for samples with and without pre-laser irradiation. The smaller values of FWHM for samples with laser irradiation indicate that quality of grown layers for samples with laser irradiation is higher than those for samples without laser irradiation. This is another significant advantage of this method over conventional SPC.

Based on these findings, we speculate the growth mechanism by weak laser irradiation and subsequent thermal annealing as shown in Fig. 4. During laser irradiation with low fluence (10-100 mJ/cm^2), a limited number of nuclei are generated by amorphicity modulation [Figs. 4(a) and 4(b)]. Subsequently, lateral growth is generated from the small amount of nuclei during thermal annealing. Here, the growth velocity significantly depends on the annealing temperature. In the case of annealing at 150 °C, laser-irradiation-induced nuclei grow so slowly that very long annealing time is required to complete crystallization. Thus, a large number of spontaneous nuclei are also generated during such long thermal annealing, which results in small grain growth [Fig. 4(c)]. This situation is almost the same as that in the conventional SPC, i.e., without laser irradiation. On the other hand, in the case of annealing at 160-200 °C, laser-irradiation-induced nuclei rapidly grow without generating spontaneous nucleation. As a result, large grains are obtained by weak laser irradiation and subsequent

thermal annealing (170-200 °C) [Fig. 4(d)]. This well explains formation of high quality GeSn films by weak laser irradiation and subsequent low temperature annealing (170-200 °C) in a short time (~5 h).

In summary, we have developed a growth technique employing weak laser irradiation and subsequent thermal annealing to obtain high quality GeSn on insulator at a low temperature in a short processing time. Low fluence irradiation (10-100 mJ/cm^2) significantly enhances SPC in subsequent thermal annealing. This enables formation of GeSn crystals at a low temperature (~170 °C) in a short annealing time (~5 h), where the quality of the grown layers are higher compared with conventional PLA or SPC. The substitutional Sn concentrations in grown layers are as high as 8-10% and shows high thermal stability. The growth mechanism based on a limited number of nucleation by weak laser irradiation and subsequent lateral SPC by thermal annealing is proposed. These methods will be useful for realization of next-generation high performance devices on flexible insulating substrate with low softening temperatures (~200 °C).

Part of this work was supported by a Grant-in-Aid (25289089, 15H03976, 16K14234) for Scientific Research from the Ministry of Education, Culture, Sports, Science, and Technology of Japan.

[1] S. Gupta, B. Magyari-Köpe, Y. Nishi, and K. Saraswat, J. Appl. Phys. **113**, 073707 (2013).
[2] S. Wirths, R. Geiger, N. von den Driesch, G. Mussler, T. Stoica, S. Mantl, Z. Ikonic, M. Luysberg, S. Chiussi, J. M. Hartmann, H. Sigg, J. Faist, D. Buca, and D. Grützmacher, Nature Photon. **9**, 88 (2015).
[3] F. Oliveira, I. A. Fischer, A. Benedetti, P. Zaumseil, M. F. Cerqueira, M. I. Vasilevskiy, S. Stefanov, S. Chiussi, and J. Schulze, Appl. Phys. Lett. **107**, 262102 (2015).
[4] S. Zaima, O. Nakatsuka, N. Taoka, M. Kurosawa, W. Takeuchi, and M. Sakashita, Sci. Technol. Adv. Mater. **16**, 043502 (2015).
[5] L. Kormoš, M. Kratzer, K. Kostecki, M. Oehme, T. Šikola, E. Kasper, J. Schulze, and C. Teichert, Surf. Interface Anal. **49**, 297 (2017).
[6] V. Schlykow, W. M. Klesse, G. Niu, N. Taoka, Y. Yamamoto, O. Skibitzki, M. R. Barget, P. Zaumseil, H. von Känel, M. A. Schubert, G. Capellini, and T. Schroeder, Appl. Phys. Lett. **109**, 202102 (2016).
[7] S. Al-Kabi, S. A. Ghetmiri, J. Margetis, W. Du, A. Mosleh, W. Dou, G. Sun, R. A. Soref, J. Tolle, B. Li, M. Mortazavi, H. A. Naseem, and S.-Q. Yu, J. Electronics Mat. **45**, 6251 (2016).
[8] A. Gassenq, L. Milord, J. Aubin, N. Pauc, K. Guilloy, J. Rothman, D. Rouchon, A. Chelnokov, J. M. Hartmann, V. Reboud, and V. Calvo, Appl. Phys. Lett. **110**, 112101 (2017).
[9] M. Miyao and T. Sadoh, Jpn. J. Appl. Phys. **56**, 05DA06 (2017).
[10] W. Takeuchi, N. Taoka, M. Kurosawa, M. Sakashita, O. Nakatsuka, and S. Zaima, Appl. Phys. Lett. **107**, 022103 (2015).
[11] H. Chikita, R. Matsumura, Y. Kai, T. Sadoh, and M. Miyao, Appl. Phys. Lett. **105**, 202112 (2014).
[12] T. Sadoh, Y. Kai, R. Matsumura, K. Moto, and M. Miyao, Appl. Phys. Lett. **109**, 232106 (2016).
[13] M. Kurosawa, N. Taoka, H. Ikenoue, O. Nakatsuka, and S. Zaima, Appl. Phys. Lett. **104**, 061901 (2014).
[14] K. Moto, R. Matsumura, T. Sadoh, H. Ikenoue, and M. Miyao, Appl. Phys. Lett. **108**, 262105 (2016).
[15] R. Matsumura, H. Chikita, Y. Kai, T. Sadoh, H. Ikenoue, and M. Miyao, Appl. Phys. Lett. **107**, 262106 (2015).
[16] R. W. Olesinski and G. J. Abbaschian, Bull. Alloy Phase Diagrams **5**, 265 (1984).
[17] J. Humlíček, M. Garriga, M. I. Alonso, and M. Cardona, J. Appl. Phys. **65**, 2827 (1989).
[18] S. Yamaguchi, N. Sugii, S. K. Park, K. Nakagawa, and M. Miyao, J. Appl. Phys. **89**, 2091 (2001).
[19] C. Spinella, S. Lombardo, and F. Priolo, J. Appl. Phys. **84**, 5383 (1998).
[20] H. Kanno, K. Toko, T. Sadoh, and M. Miyao, Appl. Phys. Lett. **89**, 182120 (2006).
[21] H. Lin, R. Chen, Y. Huo, T. I. Kamins, and J. S. Harris, Appl. Phys. Lett. **98**, 261917 (2011).
[22] M. Kurosawa, Y. Tojo, R. Matsumura, T. Sadoh, and M. Miyao, Appl. Phys. Lett. **101**, 091905 (2012).